

2023

Immunofluorescence Visualization of Polycyclic Aromatic Hydrocarbon Mixtures in the Eastern Oyster *Crassostrea virginica*

Kristen M. Prossner

Hamish J. Small

Ryan Carnegie

Michael A. Unger

Follow this and additional works at: <https://scholarworks.wm.edu/vimsarticles>



Part of the [Environmental Indicators and Impact Assessment Commons](#)

Immunofluorescence Visualization of Polycyclic Aromatic Hydrocarbon Mixtures in the Eastern Oyster *Crassostrea virginica*

Kristen M. Prossner, Hamish J. Small, Ryan B. Carnegie, and Michael A. Unger*

Virginia Institute of Marine Science, William & Mary, Gloucester Point, Virginia, USA

Abstract: Bivalve mollusks including oysters have low metabolic potential and are therefore susceptible to accumulating high levels of lipophilic organic contaminants such as polycyclic aromatic hydrocarbons (PAHs). Human exposure to PAHs via consumption of this important commercial shellfish can be a serious public health concern in areas where high PAH contamination exists. Previous PAH immunohistochemical studies have been limited to laboratory-based exposures focusing on one or a few individual PAH compounds. To date, such studies have yet to explore PAH accumulation in oysters, known to have some of the highest levels of PAHs across different food products. Using a monoclonal antibody selective for a range of three- to five-ring PAHs, we present a method to detect and localize complex mixtures of PAHs in oyster tissues via fluorescent immunohistochemistry. Observed immunofluorescence intensity followed a similar trend as measured levels of PAHs in oyster interstitial fluid from PAH-contaminated sites and oysters exposed to the water accommodated fraction of crude oil. This method will be valuable in understanding internal partitioning mechanisms of PAH-exposed oysters and will have important applications in studies on PAH distribution in the tissues of additional organisms for environmental, medical, or veterinary purposes. *Environ Toxicol Chem* 2022;00:1–6. © 2022 The Authors. *Environmental Toxicology and Chemistry* published by Wiley Periodicals LLC on behalf of SETAC.

Keywords: Polycyclic aromatic hydrocarbons (PAHs); histology; bioaccumulation; oil spills

INTRODUCTION

A class of hydrophobic organic contaminants known to have toxic and carcinogenic effects in organisms, polycyclic aromatic hydrocarbons (PAHs) exist in the environment as complex mixtures comprised of hundreds of different individual compounds (Latimer & Zheng, 2003; Lawal, 2017). As sessile, benthic fauna with limited metabolic capacity to excrete PAHs, bivalve mollusks such as oysters are highly sensitive to accumulation of this contaminant in their tissues (James, 1989). As an important commercial shellfish, oysters can also represent a potential public health hazard of human PAH exposure via consumption of contaminated oysters (European Food Safety Authority, 2008; National Oceanic and Atmospheric Administration Fisheries Eastern Oyster Biological Review Team, 2007).

The use of immunohistochemistry (IHC) has been a standard practice in medical pathology applications such as assessments of oncological biomarkers, diagnoses of diseases, as well as evaluations of neurodegenerative disorders (Dugger & Dickson, 2017; Hawes et al., 2009). Because of the known impact environmental pollutants like PAHs can have on biological health, there is a growing body of work using novel imaging technologies and IHC approaches, including immunofluorescence, for examining various mechanisms involved in biotic exposure to contaminants (Einsporn & Koehler, 2008; Lobel & Davis, 2002; Sforzini et al., 2014; Strandberg et al., 1998). However, many of these techniques have been limited in their ability to detect only one or a few individual PAH compounds via laboratory exposures (Rodríguez & Bishop, 2005; Sforzini et al., 2014; Speciale et al., 2018; Subashchandrabose et al., 2014; Wang et al., 2012). By targeting a few specific PAHs out of a contaminant class containing hundreds of compounds, such studies do not reflect real-world complex mixtures to which biota are exposed. Further, despite having some of the highest levels of PAHs relative to other food products, oysters have not served as study organisms in such IHC investigations of PAH bioaccumulation, to the authors' knowledge.

This is an open access article under the terms of the Creative Commons Attribution-NonCommercial License, which permits use, distribution and reproduction in any medium, provided the original work is properly cited and is not used for commercial purposes.

* Address correspondence to munger@vims.edu

Published online 13 December 2022 in Wiley Online Library (wileyonlinelibrary.com).

DOI: 10.1002/etc.5539

To visualize the accumulation of complex environmental PAH mixtures in eastern oysters (*Crassostrea virginica*), we employed a highly sensitive monoclonal antibody (mAb 2G8) for use in IHC techniques with demonstrated uniform selectivity for a range of three- to five-ring PAHs including both parent compounds and alkylated derivatives (Li et al., 2016). Therefore, PAHs derived from both petrogenic and pyrogenic sources are detected. The mAb 2G8 antibody was initially developed for use on the KinExA Inline Sensor (Sapidyne Instruments), a biosensing instrument that quantifies PAH concentration via the detection of fluorescently tagged antibody bound to PAHs in an aqueous sample (Li et al., 2016). Employing mAb 2G8 conjugated to the far-red fluorescent dye Alexa Fluor 647 (AF647), the biosensor has been successfully used to quantify total three- to five-ring PAH concentrations in environmental samples such as porewater (Camargo et al., 2022; Conder et al., 2021; Hartzell et al., 2017; Li et al., 2016) and oyster interstitial fluid (Prossner et al., 2022). Extending beyond its employment as a quantitative tool, we explore a novel application of AF647-tagged mAb 2G8 to observe PAH localization in oyster gill tissues using IHC techniques coupled with confocal microscopic imaging. For demonstration of this new application for the antibody, we focus our observations of mAb signal to within the water tube and plicae of the gill because we believe these exterior-facing structures to be important regions for accumulation of PAHs dissolved in the aqueous phase. We hypothesize that the incorporation of mAb 2G8 in an IHC approach will allow us to localize PAHs within tissues and that the intensity of observed fluorescent signal will be related to PAH body burden. Bioaccumulation of PAH mixtures from two different examples of oyster exposure was investigated (1) chronic exposure of wild oysters residing in historically contaminated sites in the Elizabeth River (VA, USA), and (2) acute laboratory-based exposure of oysters to the water accommodated fraction (WAF) of crude oil.

MATERIALS AND METHODS

Collection of wild Elizabeth River oysters

The Elizabeth River is a tidal urban estuary in southeast Virginia, USA, known for highly elevated levels of PAHs observed in sediment primarily due to historic pollution from several defunct wood treatment and creosote facilities in the area (Di Giulio & Clark, 2015). Six native adult *C. virginica* oysters were collected from Jones Creek, an Elizabeth River site in which elevated PAH levels have been previously observed (Prossner et al., 2022). Collected oysters were placed in coolers and returned to the laboratory, where they were stored whole (in shell) and out of water at 4 °C for 1–2 days prior to processing, to ensure that depuration did not occur.

Collection of WAF-exposed oysters

Adult aquacultured oysters purchased from an oyster farm on the York River in Gloucester County, Virginia (>80 km away from the Elizabeth River), were exposed to a constant 15- μ g/L dose

(parts per billion) of crude oil WAF for a period of 4 days, followed by a 12-day depuration period via a flow-through tank system in a PAH kinetics experiment. To dose the oysters during the uptake/depuration kinetics study, a WAF was prepared from heavy fuel oil distillate using a generator column. A large (10 \times 70 cm) generator column was packed with ignited filter sand that was coated with 40 ml of heavy fuel oil. The column was pumped at 100 ml/min with York River water in a 310-L closed recirculating system for 260 h until the total PAH concentration in the water reached steady state at 30 μ g/L total PAH. This prepared WAF was then diluted 1:1 with clean York River water to maintain an average concentration of 15 μ g/L for the duration of the 72-h dosing experiment.

Oysters were held in unfiltered York River water and not provided supplemental food. Background PAH concentration in York River water was monitored consistently throughout the experiment and averaged approximately 1 μ g/L. Animal husbandry parameters including temperature, salinity, pH, dissolved oxygen, and ammonia were maintained at appropriate levels, as outlined in ASTM standard guide E1022-94 (ASTM International, 1994). No mortality was observed throughout the experimental period. Three oysters per sampling were collected throughout the experiment at five time points: T0, pre-exposure background; T1, first day of uptake; T2, last day of uptake; T3, day 4 of depuration; T4, day 8 of depuration; and T5, day 12 (last day) of depuration. Oysters were held out of water at 4 °C for 1–2 days prior to processing, to avoid depuration. Interstitial fluid from identical oysters was preserved for biosensor analysis for corresponding PAH concentration measurement (see section *Semiquantitative image analysis*).

Sample processing

Oysters were scrubbed clean, then shucked using an oyster knife. Gill tissue fragments (~6 mm³) were dissected from each oyster and embedded in optimal cutting temperature (OCT) media within a disposable cryomold (Tissue-Tec). Embedded tissue fragments were subsequently gently frozen over a bath of liquid nitrogen-cooled pentane. Briefly, approximately 300 ml of 100% pentane was poured into a small metal bowl, which was then partially submerged in liquid nitrogen so that the pentane would reach near-freezing temperatures. The bottom of tissue-containing cryomolds was held on the surface of the near-freezing pentane so that the contents of the cryomold would gently freeze (to reduce the risk of a compromised specimen via ice crystal formation). Once frozen, the OCT-tissue blocks were stored at –80 °C. One day prior to cryosectioning, the blocks were transferred to a –20 °C freezer.

Cryosectioning and fluorescent IHC

Components of a protocol for benzo[a]pyrene localization in earthworm (*Eisenia andrei*) tissue by Sforzini et al. (2014) were adapted for use with oyster tissues and our AF647-tagged mAb 2G8. Individual tissue blocks were initially frozen to an aluminum cryostat chuck using OCT media, and 10- μ m frozen sections were

cut at 10 °C (for both the cryochamber and object temperature) using a cryostat (Leica CM3050 S). Frozen sections were directly transferred to a glass slide (Superfrost Plus; Fisher Scientific) at ambient room temperature. Tissue sections were fixed in 4% paraformaldehyde in 1× phosphate-buffered saline (PBS) for 20 min at room temperature. Fixed sections were subsequently washed in 1× PBS three times (5 min per wash) before a 1-h incubation at room temperature in a blocking and permeabilization solution containing 0.5% Triton X-100, 2% bovine serum albumin (BSA), and 0.5% rabbit serum in 1× PBS. Sections were then washed three times (as above) and incubated with the AF647-tagged 2G8 mAb (1:100 dilution in 1× PBS containing 1% BSA and 0.05% Triton X-100) overnight at 4 °C in a moist chamber. After overnight incubation, the sections were washed three times (as above), then incubated with 4',6-diamidino-2-phenylindole (DAPI), a blue fluorescent stain for DNA (to provide histoarchitectural definition to the microscopic images), at a 1:5000 dilution in 1× PBS for 15 min at room temperature. Sections were washed three times (as above) and dried, then a coverslip was mounted using Dako mounting media. On drying, clear nail varnish was applied to seal around the edges of the coverslip prior to fluorescence microscopy. Negative controls (to assess nonspecific fluorescence) consisting of tissue sections from the same individual oyster were processed in an identical manner as above but were not exposed to AF647-tagged 2G8 mAb. Sections were evaluated and images captured using a FLUOVIEW FV1200 confocal laser scanning microscope (Olympus) with filter sets for DAPI and AF647. Oyster gill tissue fragments were dissected from a separate batch of oysters collected from Jones Creek and then fixed and processed for standard paraffin histology using standard techniques. These were stained with hematoxylin and eosin dye and imaged under a standard light microscope for histoarchitectural comparison with sections processed for confocal microscopy.

Semiquantitative image analysis

Analysis of the change in integrated density of fluorescent signal in gill tissue sections of WAF-exposed oysters was

conducted using FIJI software (Schindelin et al., 2012). Integrated density is the product of total selected area and mean gray value (i.e., amount of signal in the selected image area). Because imaged gill sections varied in terms of extracellular space and intercellular cavities, three representative gill pliae per image were selected to provide standardization in measurement based on uniform scaling of the image. Measurements were repeated in triplicate to reduce random error. Analysis of variance followed by a Tukey post hoc test was conducted to compare means across different sampling time periods (T0–T5) during the WAF exposure experiment. Integrated density of the fluorescent signal was then compared with PAH concentration measured in the corresponding oyster interstitial fluid via KinExA Inline Sensor methodology (Prossner et al., 2022) to observe if a signal–concentration trend existed throughout the experiment.

RESULTS AND DISCUSSION

IHC in wild *C. virginica*

No fluorescent signal was detected in gill tissues from control sections that were processed without the inclusion of the AF647-tagged 2G8 mAb (Figure 1A). Immunofluorescence signal indicative of the presence of select three- to five-ring PAHs was observed in gill sections exposed to mAb 2G8 (Figure 1B). Specifically, intense fluorescent signal was observed in a key gill structure involved in water filtration and transportation—the water tube (Eble & Scro, 1996). Localization in the water tube was confirmed through comparison with a hematoxylin and eosin–stained gill tissue section, which provides a more refined image of the target gill structures (Figure 1C). The accumulation of PAHs and thus intense mAb 2G8 signal primarily along the lipid membrane of these gill structures is reasonable because the lipid in this region serves as a first point of contact for these lipophilic molecules on entering the oyster gill. Although fluorescence is observed mainly within the external regions of the gill, due in part to the focus of our study, we still interpret this as localization of PAH distributed within tissue, not solely bound to the tissue surface.

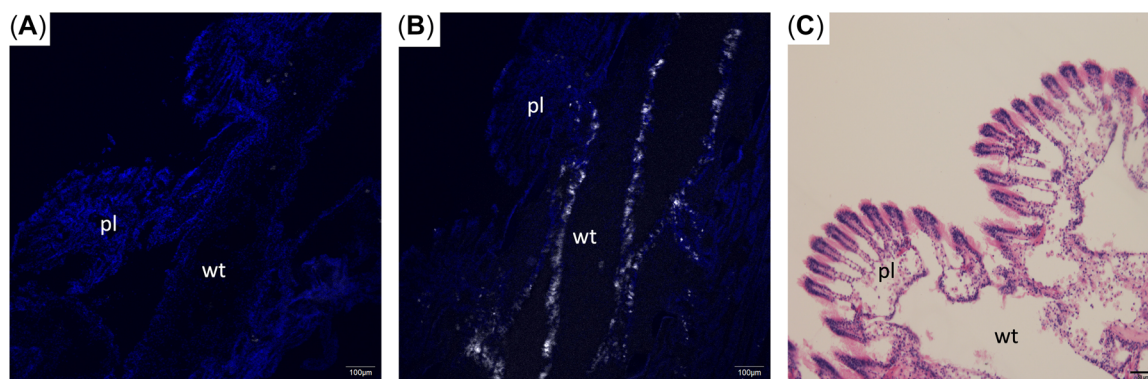


FIGURE 1: Representative images of immunofluorescence detection of three- to five-ring polycyclic aromatic hydrocarbons (PAHs) in gill tissue of a wild Elizabeth River oyster. (A) Negative control not exposed to 2G8 monoclonal antibody; (B) immunofluorescence detection of PAHs (white signal) in gill structures; (C) hematoxylin and eosin–stained gill section from native Elizabeth River oyster from the same site with more refined histo-architecture for comparison (note scale change). Staining in (A) and (B) is with 4',6-diamidino-2-phenylindole for cell nuclei (blue signal). pl = plicae; wt = water tube.

Observation of fluorescence in 1- μm slices of the images through the z-axis via z-stack analysis on the confocal microscope, with maximum fluorescence observed in the middle slice, supports our interpretation. In addition, the use of Triton X-100 in the described IHC protocol permeabilizes eukaryotic cell membranes and facilitates mAb 2G8 binding to intracellular PAH.

IHC and PAH quantification in WAF-exposed *C. virginica*

Exposing oysters to WAF in a PAH kinetics study provided an ideal opportunity to examine time-dependent dose and its effect on tissue concentrations and imaging. Imaging of gill tissue collected from WAF-exposed oysters allowed for comparison of mAb 2G8 fluorescent signal to accumulated PAH concentrations through time (Figures 2 and 3). Overall, IHC staining of gill structures in laboratory-exposed oysters (Figure 2A–F) was similar to that in chronically exposed native oysters (Figure 1A–C); however, a stronger signal was observed in the plicae of the laboratory-exposed oysters, another important gill structure for water filtration and transportation (Eble & Scro, 1996). Due to the ubiquity of PAHs in the environment, the susceptibility of oysters to accumulation, and the sensitivity of mAb 2G8, fluorescent signal indicative of low levels of PAHs was observed in preexposure background oysters (Figure 2A).

On the first day of exposure, T1 (Figure 2B), a stronger signal relative to T0 (Figure 2A) was observed, which can be attributed to the capacity of oysters to filter large volumes of water (0.12 m³ g⁻¹ dry wt/day or ~50 gallons or ~190 L of water per day for an individual oyster; Newell, 1988). Thus, oysters can rapidly concentrate environmental contaminants such as PAHs. The highest PAH signal intensity was observed on the final day of uptake (T2; Figure 2C) and steadily decreased throughout the depuration period (Figure 2D,E). By the last day of depuration, T5 (Figure 2F), fluorescent signal for PAH had returned to nearly the same levels observed at T0 (Figure 2A). Notably, the two PAH mixtures employed as sources of exposure for the present study vary greatly in PAH composition: Creosote, the predominant source of PAH pollution in the Elizabeth River, is comprised primarily of pyrogenic PAHs, whereas the heavy fuel oil WAF consists of mostly petrogenic PAHs (Neff et al., 2005). Through successful imaging of fluorescent signal in oysters exposed to different PAH sources via a mAb uniformly selective for a wide range of PAH compounds, we demonstrate the versatility of mAb 2G8 for future imaging applications.

Overall, the level of integrated density of specific fluorescent signal for PAHs (AF647-tagged 2G8 mAb; Figure 3A) measured in gill tissue images (Figure 2A–F) followed a similar trend as the PAH concentration measured in the interstitial fluid of the identical oyster (Figure 3B). An analysis of variance yielded a significant difference ($F=40.0$, $df=5$, $p<0.05$) in integrated density of signal across the different time points of

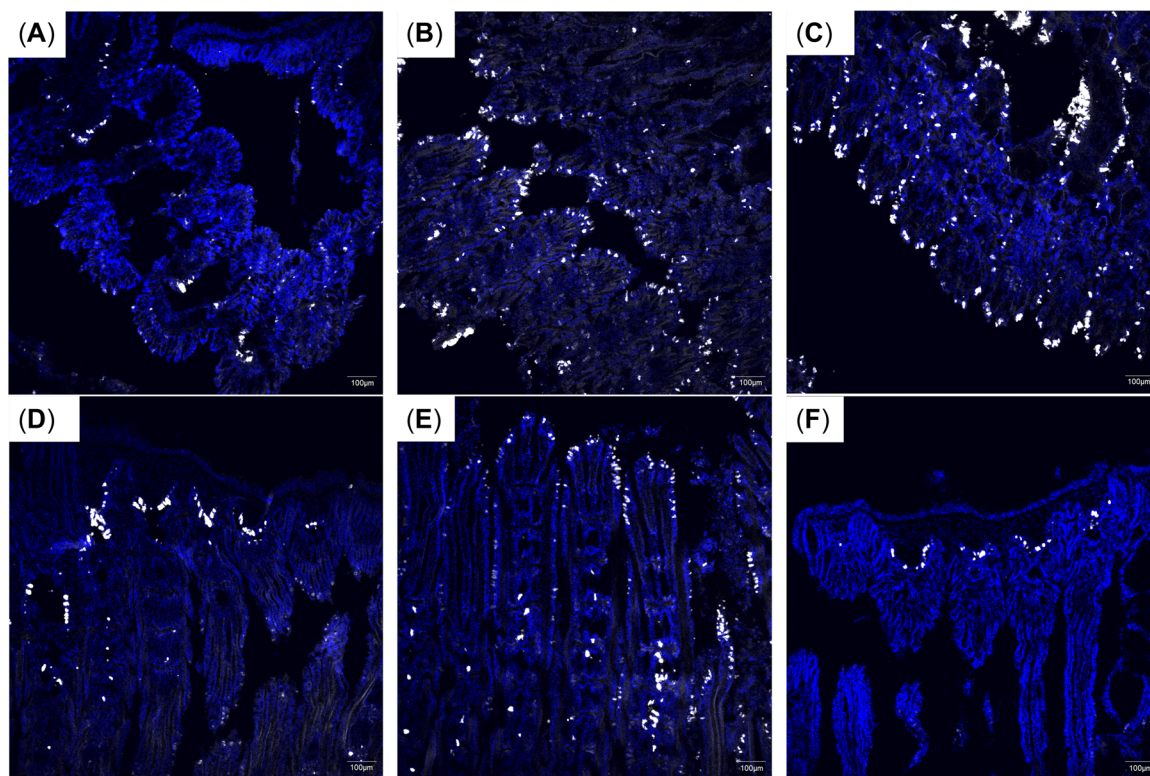


FIGURE 2: Representative images of immunofluorescence detection of polycyclic aromatic hydrocarbon (PAH) by monoclonal antibody 2G8 in gill sections from oysters sampled at different time points throughout a 16-day laboratory crude oil water accommodated fraction exposure: (A) = T0, background (pre-exposure); (B) = T1, first day uptake; (C) = T2, last day uptake; (D) = T3, day 4 depuration; (E) = T4, day 8 depuration; and (F) = T5, final day of depuration. Sections were also stained with 4',6-diamidino-2-phenylindole (blue signal).

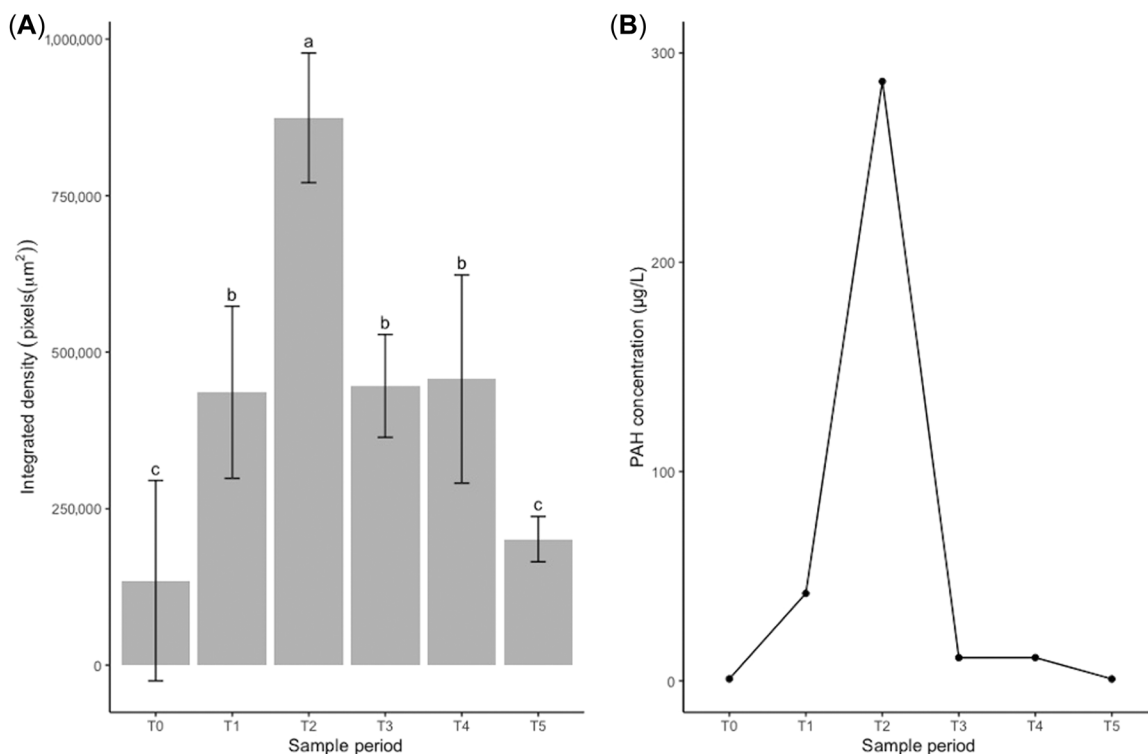


FIGURE 3: Comparison of (A) image integrated density in representative oyster gill tissue images (Figure 2) across sampling periods during a crude oil water accommodated fraction exposure experiment to (B) corresponding polycyclic aromatic hydrocarbon concentrations measured in interstitial fluid of identical oysters (Prossner et al., 2022). Error bars depict the standard deviation. Letters depict groupings of specific significant differences across sampling periods determined via Tukey post hoc testing. Sample periods with the same letter are not significantly different from each other but are different from groups with a different letter. PAH = polycyclic aromatic hydrocarbon.

the experiment. Through Tukey post hoc testing, it was determined that T2, the final day of uptake and the highest PAH concentration, was significantly different from all other sampling periods. Periods T1, T3, and T4 were not significantly different from each other but were significantly different from T0 and T5, the final day of depuration. Periods T0 and T5 were also not significantly different from each other. Groupings of specific significant differences across sampling periods are reported in Figure 3A. Through semiquantitative analysis, we found that the change in intensity of fluorescent signal observed throughout the experiment is related to PAH body burden measured at corresponding time points. This suggests that mAb 2G8 can be used not only as a visualization tool to localize where PAHs accumulate in tissue but also to observe the relative distribution of PAHs within the tissues. We determined that a similar general trend between signal and tissue concentration exists, supporting the future direction of the technique to compare relative concentration gradients within biological tissues (e.g., PAH distribution in gills relative to digestive gland) as well as providing additional evidence of PAH selectivity of the antibody. To describe a more specific correlative relationship between signal and tissue concentration, more in-depth quantitative analysis is needed, which is neither within the scope of this initial study nor an intended objective. We do not intend for this new application of mAb 2G8 to serve as a quantitative tool to predict tissue concentrations but, instead, to allow for a more in-depth understanding of

accumulation and distribution of complex PAH mixtures in tissue via immunofluorescence.

CONCLUSION

In the present study, we demonstrate the application of a PAH mAb for use in IHC techniques to detect and localize accumulation of two complex PAH mixtures with differing PAH compositions in biotic tissue. To our knowledge, this is the first IHC study of PAH accumulation in oysters—a potentially important source of PAH exposure for humans via consumption following contamination events such as oil spills. Although gill tissue was the focus of the present study, we plan to explore PAH accumulation in other tissues using this technique. The signal detected using the AF647-tagged mAb 2G8 reflects more realistic levels of exposure experienced by organisms than what can be analyzed using current techniques for visualizing exposure of one or a few individual PAHs. In addition, as known carcinogens, the ability to localize and visualize exposure to PAH mixtures in tissue may have important medical or veterinary applications. Demonstrating that the PAH signal intensity via image analysis is related to PAH body burden, we also predict that mAb 2G8 can help evaluate important environmental and biological partitioning mechanisms, which will be a target for future research.

Acknowledgment—We wish to thank the following Virginia Institute of Marine Science researchers for their contributions: M. Mainor, M. A. Vogelbein, and F. Knight for field and laboratory assistance, as well as R. Crockett and M. Kolacy for histology assistance. We also thank the reviewers for helpful comments. The present study was supported through ExxonMobil Biomedical Sciences, Inc., and the Virginia Institute of Marine Science.

Conflict of Interest—The authors declare no conflict of interest.

Author Contributions Statement—**Kristen M. Prossner**: Writing—original draft; Investigation; Methodology; Formal analysis; Data curation; Conceptualization; Visualization. **Hamish J. Small**: Investigation; Conceptualization; Methodology; Formal analysis; Supervision; Writing—review & editing. **Ryan B. Carnegie**: Investigation; Supervision; Writing—review & editing. **Michael A. Unger**: Investigation; Resources; Conceptualization; Supervision; Funding acquisition; Writing—review & editing.

Data Availability Statement—The main data produced in our study are the images, and they are included in the article. Data are also available from the authors on request (munger@vims.edu).

REFERENCES

- ASTM International. (1994). Standard guide for conducting bioconcentration tests with fishes and saltwater bivalve mollusks. In *Annual book of standards* (Vol. 11.04, E1022–94).
- Camargo, K., Vogelbein, M. A., Horney, J. A., Dellapenna, T. M., Knap, A. H., Sericano, J. L., Wade, T. L., McDonald, T. J., Chiu, W. A., & Unger, M. A. (2022). Biosensor applications in contaminated estuaries: Implications for disaster research response. *Environmental Research*, 204, Article 111893.
- Conder, J., Jalalizadeh, M., Luo, H., Bess, A., Sande, S., Healey, M., & Unger, M. A. (2021). Evaluation of a rapid biosensor tool for measuring PAH availability in petroleum-impacted sediment. *Environmental Advances*, 3, Article 100032.
- Di Giulio, R. T., & Clark, B. W. (2015). The Elizabeth River story: A case study in evolutionary toxicology. *Journal of Toxicology and Environmental Health, Part B*, 18(6), 259–298.
- Dugger, B. N., & Dickson, D. W. (2017). Pathology of neurodegenerative diseases. *Cold Spring Harbor Perspectives in Biology*, 9(7), Article a028035.
- Eble, A. F., & Scro, R. (1996). General anatomy. In V. S. Kennedy, R. I. E. Newell, & A. F. Eble (Eds.), *The eastern oyster: Crassostrea virginica* (pp. 19–30). Maryland Sea Grant College.
- Einsporn, S., & Koehler, A. (2008). Immuno-localisations (GSSP) of sub-cellular accumulation sites of phenanthrene, aroclor 1254 and lead (Pb) in relation to cytopathologies in the gills and digestive gland of the mussel *Mytilus edulis*. *Marine Environmental Research*, 66(1), 185–186.
- European Food Safety Authority. (2008). Scientific opinion of the panel on contaminants in the food chain on a request from the European Commission on polycyclic aromatic hydrocarbons in food. *The EFSA Journal*, 724, 1–114.
- Hartzell, S. E., Unger, M. A., McGee, B. L., & Yonkos, L. T. (2017). Effects-based spatial assessment of contaminated estuarine sediments from Bear Creek, Baltimore Harbor, MD, USA. *Environmental Science and Pollution Research*, 24(28), 22158–22172.
- Hawes, D., Shi, S. R., Dabbs, D. J., Taylor, C. R., & Cote, R. J. (2009). Immunohistochemistry. In N. Weidner, R. J. Cote, S. Suster, & L. M. Weiss (Eds.), *Modern surgical pathology* (Vol. 1, pp. 48–70). Elsevier.
- James, M. (1989). Biotransformation and disposition of PAH in aquatic invertebrates. In U. Varanasi (Ed.), *Metabolism of polycyclic aromatic hydrocarbons in the aquatic environment* (pp. 69–92). CRC.
- Lobel, L. M. K., & Davis, E. A. (2002). Immunohistochemical detection of polychlorinated biphenyls in field collected damselfish (*Abudefduf sordidus*; Pomacentridae) embryos and larvae. *Environmental Pollution*, 120(3), 529–532.
- Latimer, J., & Zheng, J. (2003). The sources, transport, and fate of PAHs in the marine environment. In P. E. T. Douben (Ed.), *PAHs: An ecotoxicological perspective* (pp. 7–33). Wiley.
- Lawal, A. T. (2017). Polycyclic aromatic hydrocarbons. A review. *Cogent Environmental Science*, 3(1), Article 1339841.
- Li, X., Kaattari, S. L., Vogelbein, M. A., Vadas, G. G., & Unger, M. A. (2016). A highly sensitive monoclonal antibody based biosensor for quantifying 3–5 ring polycyclic aromatic hydrocarbons (PAHs) in aqueous environmental samples. *Sensing and Bio-Sensing Research*, 7, 115–120.
- National Oceanic and Atmospheric Administration Fisheries Eastern Oyster Biological Review Team. (2007). *Status review of the eastern oyster (Crassostrea virginica). Report to the National Marine Fisheries Service (NOAA Technical Memo NMFS F/SPO-88)*. National Marine Fisheries Service.
- Neff, J. M., Stout, S. A., & Gunster, D. G. (2005). Ecological risk assessment of polycyclic aromatic hydrocarbons in sediments: Identifying sources and ecological hazard. *Integrated Environmental Assessment and Management*, 1(1), 22–33.
- Newell, R. (1988, August). Ecological changes in Chesapeake Bay: Are they the result of over-harvesting the American oyster, *Crassostrea virginica*? In M. P. Lynch & E. C. Krome (Eds.), *Understanding the estuary: Advances in Chesapeake Bay research* (pp. 536–546). Chesapeake Bay Consortium.
- Prossner, K. M., Vadas, G. G., Harvey, E., & Unger, M. A. (2022). A novel antibody-based biosensor method for the rapid measurement of PAH contamination in oysters. *Environmental Technology & Innovation*, 28, Article 102567.
- Rodríguez, S. J., & Bishop, P. L. (2005). Competitive metabolism of polycyclic aromatic hydrocarbon (PAH) mixtures in porous media biofilms. *Water Science and Technology*, 52(7), 27–34.
- Schindelin, J., Arganda-Carreras, I., Frise, E., Kaynig, V., Longair, M., Pietzsch, T., & Cardona, A. (2012). Fiji: An open-source platform for biological-image analysis. *Nature Methods*, 9(7), 676–682. <https://doi.org/10.1038/nmeth.2019>
- Sforzini, S., Moore, M. N., Boeri, M., Benfenati, E., Colombo, A., & Viarengo, A. (2014). Immunofluorescence detection and localization of B[a]P and TCDD in earthworm tissues. *Chemosphere*, 107, 282–289.
- Speciale, A., Zena, R., Calabrò, C., Bertuccio, C., Aragona, M., Saija, A., & Cascio, P. L. (2018). Experimental exposure of blue mussels (*Mytilus galloprovincialis*) to high levels of benzo[a]pyrene and possible implications for human health. *Ecotoxicology and Environmental Safety*, 150, 96–103.
- Strandberg, J. D., Rosenfield, J., Berzins, I. K., & Reinisch, C. L. (1998). Specific localization of polychlorinated biphenyls in clams (*Mya arenaria*) from environmentally impacted sites. *Aquatic Toxicology*, 41(4), 343–354.
- Subashchandrabose, S. R., Krishnan, K., Gratton, E., Megharaj, M., & Naidu, R. (2014). Potential of fluorescence imaging techniques to monitor mutagenic PAH uptake by microalga. *Environmental Science & Technology*, 48(16), 9152–9160.
- Wang, P., Wu, T. H., & Zhang, Y. (2012). Monitoring and visualizing of PAHs into mangrove plant by two-photon laser confocal scanning microscopy. *Marine Pollution Bulletin*, 64(8), 1654–1658.